LITERATURE CITED

1. S. M. Belotserkovskii, "Computation of the flow around wings of arbitrary planform in a broad range of angles of attack," Izv. Akad. Nauk SSSR, Mekh. Zhidk. Gaza, No. 4 (1968).
2. N. F. Vorob'ev and G. N. Shashkina, "Numerical modeling of conditions for vortex sheet convergence with the wing edges," Aerodynamic Problems of Bodies of Three-Dimensional Configuration [in Russian], Inst. Teor. Prikl, Mekh., Sib. Otd. Akad. Nauk SSSR, Novosibirsk (1982).
3. N. F. Vorob'ev and G. N. Shashkina, "On the question of selecting a discrete vortex scheme," Problems of Flow around Bodies of Three-Dimensional Configuration [in Russian], Inst. Teor. Prikl. Mekh., Sib. Otd. Akad. Nauk SSSR, Novosibirsk (1978).
4. N. F. Vorov'ev and G. N. Shashkina, "Analysis of the flow around rectangular wings and their combinations in a subsonic stream by a discrete vortex scheme," Zh. Prikl. Mekh. Tekh. Fiz., No. 2 (1983).
5. N. E. Kochin, Vector Calculus and Tensor Calculus Principles [in Russian], Nauka, Moscow (1965).
6. N. F. Vorob'ev, "On a discrete vortex scheme of a finite span wing," Izv. Sib. Otd. Akad. Nauk SSSR, Ser. Tekh. Nauk, No. 13, Issue 3 (1972).
7. S. D. Ermolenko, Yu. A. Rogozin, et al., "Modeling of a flying vehicle by a thin planar surface with its projection as planform," Uch. Zap. TsAGI, 10, No. 2 (1979).

HEAT TRANSFER IN LAVAL NOZZLES WHEN A SCREEN IS PRESENT

E. P. Volchkov, V. P. Lebedev, and A. N. Yadykin

UDC 536.242

We present the results of an investigation of heat exchange when a screen is present and under complicated flow conditions: an accelerated, compressible, axisymmetric stream with compression shocks.

The tests were made on an exerimental installation described in detail in [1]. The working sections of the installation were interchangeable, supersonic, conical nozzles. The subcritical part of the nozzles had the same geometry: diameters of entrance and critical cross sections 80 and 20 mm, convergence half-angle $\varphi_1/2 = 30°$. The supersonic parts of the nozzles differed in the expansion angles, which had values of $\varphi_2/2 = 6, 30, 40°$. To measure the wall temperature, thermocouples 0.2 mm in diameter were imbedded flush with the inner surface along a generating line of the nozzle. Openings 0.4 mm in diameter for measuring the static pressure were drilled in the same cross sections where the thermocouples were mounted.

In the tests the heat flux was directed from the wall to the main air stream, having a stagnation temperature $T_0 \approx 288°K$. To increase the accuracy of the experimental determination of the heat-exchange coefficient, we developed a special method of wall heating [2], aimed at considerably reducing the heat leaks. Its essence consists of the following. A graphite-based liquid mixture was deposited in a uniform layer onto a section, consisting of a strip with a constant width of 30 mm, of the inner surface of the textolite nozzle. After drying, a thin electrically conducting film ~ 40 μm thick was formed on the wall. It was heated by passing an electric current through it, and the amount of heat released was determined from the measured power. The heat-flux density was found from the ratio of this heat to the area of the film. Since the film had a constant width and uniform heat release, the heat-flux density was constant along its length. The uniformity of heat release was monitored by the constancy of the electric resistance of individual sections of the film and by equality of the film temperature when it was heated by a current under conditions of the absence of convective heat exchange.

Because of the low thermal conductivity of the nozzle wall and of the thin electrically heated layer, the longitudinal heat leaks are small, which is especially important under the conditions of large temperature gradients in the direction of the x axis which occurred in

Novosibirsk. Translated from Zhurnal Prikladnoi Mekhaniki i Tekhnicheskoi Fiziki, No. 5, pp. 51-55, September-October, 1985. Original article submitted June 20, 1984.

0021-8944/85/2605-0648$09.50

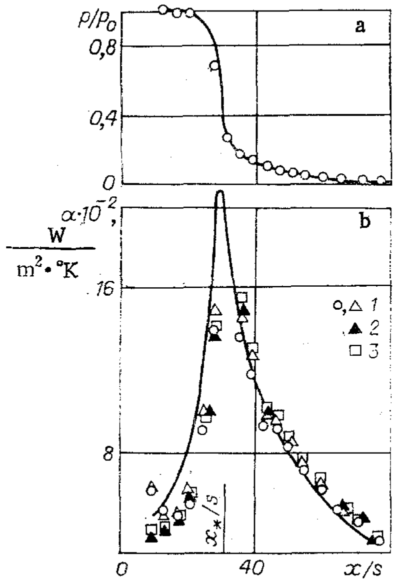

Fig. 1

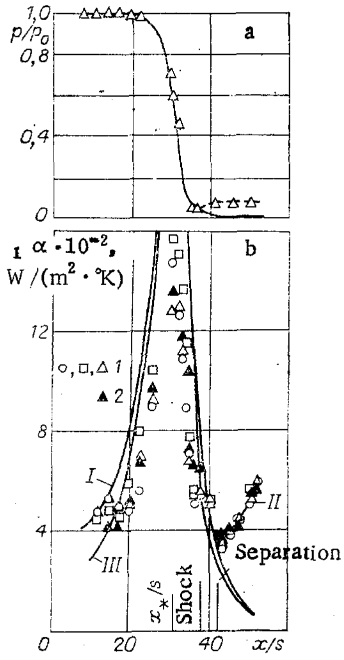

Fig. 2

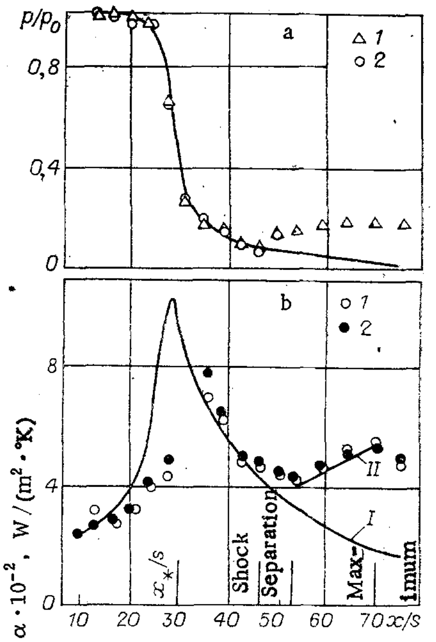

Fig. 3

the Laval nozzle. According to the measurements made, the heat leaks along the wall did not exceed 0.3%.

The screen was organized by injecting heated air ($T_s \approx 329°K$) through a tangential slot with a height s = 2.7 mm located at the entrance to the nozzle.

The experiments were carried out with a relative velocity of injection through the slot $m = \rho_s w_s/\rho_0 w_0 = 0$–$0.22$, a stagnation pressure in the forechamber $p_0 = 2 \cdot 10^5$–$8.3 \cdot 10^5$ Pa, and a constant heat flux along the wall, which had values of $q_w = 9.2 \cdot 10^3$–$17.9 \cdot 10^3$ W/m^2 in different tests. The calculated Mach number at the nozzle cut was M = 3.4. The flow regimes (rated and unrated) in the nozzles were established by varying the stagnation pressure in the forechamber and the expansion angles of the supersonic part.

In the rated flow regimes the relative variation of the static pressure p/p_0 at the wall (Fig. 1a) is described satisfactorily by a calculation for one-dimensional isentropic flow (curved line) through the equation [3]

$$\left(\frac{p}{p_0}\right)^{\frac{1}{k}}\left[1-\left(\frac{p}{p_0}\right)^{\frac{k-1}{k}}\right]^{\frac{1}{2}}=\left(\frac{k-1}{2}\right)^{\frac{1}{2}}\left(\frac{2}{k+1}\right)^{\frac{k+1}{2(k-1)}}\frac{F_*}{F}, \qquad (1)$$

where F and F_* are the areas of the current and critical cross sections; k is the adiabatic index. In Fig. 1b we present the distribution of the heat-transfer coefficient in a 30-6° nozzle for rated regimes of flow ($p_0 = 8.3 \cdot 10^5$ Pa), obtained both in the absence of a gas screen (points 1: $c_w = 13.8 \cdot 10^3$ W/m^2, m = 0) and with it present (points 2: $q_w = 13.8 \cdot 10^3$ W/m^2, m = 0.22; 3: $q_w = 9.2 \cdot 10^3$ W/m^2, m = 0.22). Here the heat-transfer coefficients in the tests with a screen were found from the measured heat-flux density at the wall and the difference between the actual and adiabatic wall temperatures. The adiabatic wall temperature was determined in tests with a screen in the absence of a heat flux at the wall. In tests without a screen the adiabatic wall temperature was equal to the equilibrium temperature. In this treatment the tests with a screen agree well with the tests without a screen. Such agreement of the heat-transfer coefficients makes it possible, in calculating the heat exchange under the conditions of a screen, to use the equations adopted in the calculations of heat exchange without a screen, in which the difference between the actual and the adiabatic wall temperatures is taken as the determining quantity.

In Fig. 1b we present a calculation of the heat-exchange coefficients made with allowance for the compressibility (Ψ_M) and nonisothermicity (Ψ_T) of the gas [4] through the equation

$$\alpha = \rho_0 w_0 c_{p_0} \Psi_T \Psi_M \left(0.0128/\mathrm{Re}_T^{**0.25}\mathrm{Pr}^{0.75}\right)(\mu_w/\mu_0)^{0.25}, \qquad (2)$$

where

$$\Psi_M = \left[\left(\operatorname{arctg} M \sqrt{r\frac{k-1}{2}}\right)\Big/ M\sqrt{r\frac{k-1}{2}}\right]^2; \quad \Psi_T = \left(\frac{2}{\sqrt{T_w/T_w^*}+1}\right)^2.$$

The Reynolds number Re_T^{**} is determined from the integral energy equation for axisymmetric flow in a nozzle,

$$\mathrm{Re}_T^{**} = \left(\int_0^x q_w D dx\right)\Big/ \mu_0 c_{p_0}(T_w - T_w^*) D,$$

where T_w is the actual wall temperature [in the presence of heat exchange ($q_w \neq 0$) and a screen]; T_w^* is the adiabatic wall temperature [in the absence of heat exchange ($q_w = 0$) and in the presence of a screen]; D is the current nozzle diameter; x is the distance along a generating line of the nozzle; μ_0 and c_{p_0} are the dynamic viscosity and heat capacity of the main stream; $\rho_0 w_0$ is the mass velocity of the stream in the current cross section.

The satisfactory agreement between experiment and calculation, especially in the supersonic part of the nozzle, is seen from Fig. 1b. The decrease in the experimental values of the heat-exchange coefficient in comparison with the calculated values in the subsonic region can be explained by laminarization of the flow under conditions of stream acceleration. In these tests the acceleration parameter $K = (\mu/\rho_0 w_0^2)/(dw_0/dz)$ exceeded the value of $K = (2-3) \cdot 10^{-6}$ at which laminarization of flow in nozzles sets in [5].

In unrated flows in regimes of overexpansion of the stream in the supersonic part of the nozzle compression shocks are formed, characterized by an increase in the static pressure at the wall. The distribution of static pressure for such flow regimes is shown in Figs. 2a-4a for nozzles with different expansion angles and different positions of the shocks (as a function of the stagnation pressure in the forechamber). In Fig. 2a $\varphi_2/2 = 40°$, $p_0 = 8.3 \cdot 10^5$ Pa, $q_w = 0$; in Fig. 3a $\varphi_2/2 = 6°$, $p_0 = 3.4 \cdot 10^5$ Pa, points 1, 2: $q_w = 0$, $9.2 \cdot 10^3$ W/m^2; in Fig. 4a $\varphi_2/2 = 6°$, $p_0 = 2 \cdot 10^5$ Pa, points 1-3: $q_w = 0$, $9.2 \cdot 10^3$, $13.8 \cdot 10^3$ W/m^2; curves: calculation for one-dimensional isentropic flow from Eq. (1).

The start of the region of interaction of the compression shocks with the boundary layer can be found from the ratio of the static pressures in this cross section and at the nozzle cut (p_{sh}/p_a), which depends on the pressure drop in the nozzle (p_0/p_a). In the literature there are a number functions for finding p_{sh}. For example, in [6]

$$\frac{p_{sh}}{p_a} = \frac{2}{3}\left(\frac{p_0}{p_a}\right)^{-0,2} \quad \text{or} \quad \pi(\lambda)_{sh} = \frac{p_{sh}}{p_0} = \frac{2}{3}\left(\frac{p_a}{p_0}\right)^{1,2}, \tag{3}$$

where p_{sh} is the pressure ahead of the compression shock, which corresponds to rated isentropic flow; p_0 is the stagnation pressure at the nozzle entrance; p_a is the pressure at the nozzle cut (or the pressure in the ambient medium).

In these experiments the static pressure p_{sh} ahead of the shock is in satisfactory agreement with the rated value calculated from Eq. (3). The cross section corresponding to the start of the region of interaction of the compression shock with the boundary layer was found using the gas-dynamic function $q(\lambda)_{sh} = F_*/F_{sh}$ and Eq. (3).

The interaction of shocks with a boundary layer can lead to separation of the stream from the wall and intensification of heat exchange. When the shock lies near the nozzle cut, air from the ambient medium is ejected into the region beyond the compression shock. At lower pressure drops (p_0/p_a) the shock wave into the interior of the nozzle, moving away from the exit cross section, and in this case air ejection from the ambient medium cannot occur. As the data of [7, 8] show, the process of heat exchange beyond a compression shock during flow without ejection is qualitatively altered and is the most complex.

In our tests in all the unrated regimes the flow can be treated as taking place without air ejection from the external medium, since the outflow takes place into a long cylindrical channel ($l/d = 30-60$). The test data on heat exchange in the region of compression shocks for nozzles with different expansion angles and different positions of the shock are shown in Figs. 2b-4b. These experiments correspond to the pressure distributions presented in Figs. 2a-4a. In Fig. 2b $\varphi_2/2 = 40°$, $p_0 = 8.3 \cdot 10^5$ Pa, points 1, 2: $m = 0$, 0.22, $q_w = 17.9 \cdot 10^3$ W/m^2; in Fig. 3b $\varphi_2/2 = 6°$, $p_0 = 3.4 \cdot 10^5$ Pa, $q_w = 9.2 \cdot 10^3$ W/m^2, points 1, 2: $m = 0$, 0.22; in Fig. 4b $\varphi_2/2 = 6°$, $p_0 = 2 \cdot 10^5$ Pa, points 1-3: $m = 0$, 0, 0.21, $q_w = 13.8 \cdot 10^3$, $9.2 \cdot 10^3$ W/m^2. The

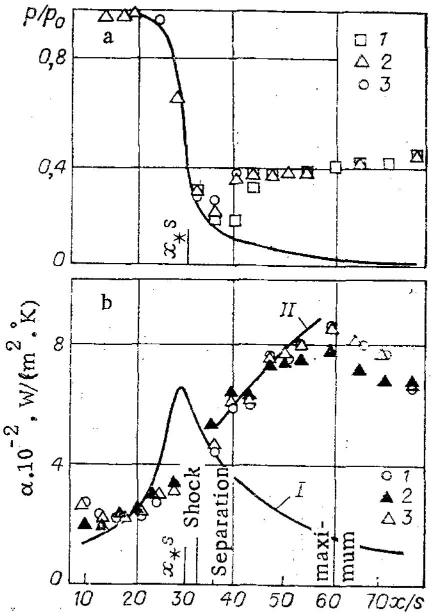

Fig. 4

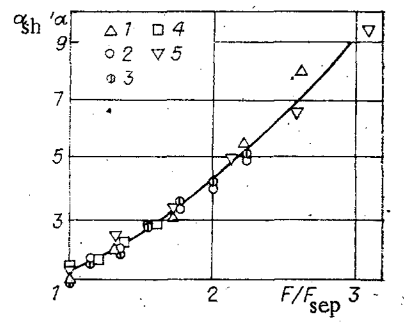

Fig. 5

heat-transfer coefficients with a gas screen present were determined from the adiabatic wall temperature. In such a treatment they coincide with the heat-transfer coefficients without a screen. In Figs. 2-4 curve I represents the calculation for the corresponding nonseparation regime of flow from Eq. (2); in Fig. 2b we also give a calculation from Bartz's equation (curve III) for calculating heat transfer in a nozzle [9],

$$\alpha = 0.026\,(\rho' w_0 D/\mu')^{0.8}\,\mathrm{Pr}'^{0.4}\,(\lambda'/D). \tag{4}$$

A prime denotes parameters determined at the characteristic temperature

$$T' = T + 0.5\,(T_w - T) + 0.22\,(T_0^+ - T),$$

where T_w is the wall temperature in the presence of heat exchange; T is the thermodynamic temperature in the core of the stream; $T_0^+ = T_0[1 + r(k-1)M^2/2]/[1 + (k-1)M^2/2]$ is the equilibrium wall temperature.

From an analysis of the experimental data obtained it follows that in the region of the shocks the rise in the heat-transfer coefficients occurs not with that cross section where an increase in static pressure is observed, but somewhat downstream. The character of variation of α can be explained by the well-known conservativity of heat exchange against a pressure gradient in a region of compression of the boundary layer up to the separation point. The small increase in α in this region comprises an average of 20%. Then one observes a strong increase in α (compared with rated flow) up to the maximum value, after which the heat-transfer coefficient starts to decrease. In certain separation regimes of flow the maximum values of the heat-transfer coefficient can even exceed the calculated values of α at the critical cross section. This pertains to cases when the compression shocks are located near the nozzle "throat," i.e., at low values of the pressure in the forechamber (or at small pressure drops p_0/p_a). The distribution of the heat-transfer coefficient in this type of flow can be seen, e.g., in Fig. 4b. As follows from the test data of [8], in a nozzle with $\varphi_2 > 8°$ the maximum value of the heat-transfer coefficient lies in the cross section with a nominal Mach number of $M = M_{sh} + 1$, where M_{sh} is the Mach number ahead of the shock.

From an analysis of our test data for different nozzle expansion angles and different positions of the shocks it follows that the ratio of the area F_{sep} of the nozzle cross section at which the heat-transfer coefficient starts to rise to the area F_{sh} of the cross section in which the pressure increase starts varies insignificantly ($F_{sep}/F_{sh} = 1.28$–1.37).

From the separation point up to the point with α_{max} the increase in the heat-transfer coefficient (relative to α for rated flow) depends on the expansion ratio F/F_{sep} of the nozzle. In Fig. 5 we present the dependence of the relative heat-transfer coefficient in the region of compression shocks on the expansion ratio of the nozzle beyond the separation cross section F_{sep} (α and α_{sh} are the heat-transfer coefficients in the rated and unrated regimes of flow). The following notation is adopted in the graph: 1) $\varphi_2/2 = 40°$, $p_0 = 8.4 \cdot 10^5$ Pa,

$q_w = 17.9 \cdot 10^3$ W/m^2; 2) $\varphi_2/2 = 6°$, $p_0 = 2 \cdot 10^5$ Pa, $q_w = 9.2 \cdot 10^3$ W/m^2; 3) $\varphi_2/2 = 6°$, $p_0 = 2 \cdot 10^5$ Pa, $q_w = 13.8 \cdot 10^3$ W/m^2; 4) $\varphi_2/2 = 6°$, $p_0 = 3.4 \cdot 10^5$ Pa, $q_w = 9.2 \cdot 10^3$ W/m^2; 5) $\varphi_2/2 = 30°$, $p_0 = 2 \cdot 10^5$ Pa, $q_w = 9.2 \cdot 10^3$ W/m^2. In such a treatment we were able to generalize the experimental results for different geometries of the supersonic part of the nozzles ($\varphi_2/2 = 6, 30, 40°$) and different positions of the compression shocks ($x_{sep}/x_* = 1.1$–1.8). The empirical function which describes the test data has the form

$$\alpha_{\text{ск}}/\alpha = 1.2(F/F_{sep})^{1.85}. \qquad (5)$$

On the basis of the generalization obtained, one can estimate the convective heat exchange in the region of interaction of compression shocks with the boundary layer from the separation point to the cross section with the maximum α. The cross section F_{sh} of the start of the region of interaction of a compression shock with the boundary layer is found from Eq. (3). Then the cross section where separation occurs is determined from $F_{sep}/F_{sh} \approx 1.3$. The heat-transfer coefficients α corresponding to the rated regime of flow in the region of $F_{sep} < F < F_{max}$ are found from Eq. (2) or (4), and then the values of the heat-transfer coefficient α_{sh} in the separation region being sought are found from Eq. (5). A calculation of the heat-transfer coefficients by the proposed method is presented in Figs. 2b-4b (curves II). It is in satisfactory agreement with the tests in the investigated range of the parameters.

LITERATURE CITED

1. É. P. Volchkov, V. K. Koz'menko, and V. P. Lebedev, "Experimental investigation of the efficiency of a gas screen in a supersonic axisymmetric nozzle," Izv. Sib. Otd. Akad. Nauk SSSR, Ser. Tekh. Nauk, Issue 2, No. 8 (1977).
2. É. P. Volchkov, V. P. Lebedev, and A. N. Yadykin, "Heat exchange in an unrated regime of flow with a screen in a Laval nozzle," in: Heat and Mass Exchange VI [in Russian], Vol. 1 (1980), Part 1.
3. O. S. Zelenkov and A. V. Yurkov, "Experimental investigation of stream separation in overexpanded conical nozzles," Uch. Zap. Leningr. Gos. Univ., No. 338 (1968).
4. S. S. Kutateladze and A. I. Leont'ev, Heat-Mass Transfer and Friction in a Turbulent Boundary Layer [in Russian], Énergiya, Moscow (1972); NASA, Washington, D.C. (1974).
5. L. H. Back and R. F. Cuffel, "Turbulent boundary layer and heat transfer measurements along a convergent nozzle," Trans. ASME, J. Heat Transfer, No. 11 (1971).
6. S. Colt and L. Bell, "Characteristics of a conical nozzle in flow with separation from the wall," Vopr. Raket. Tekh., No. 3 (1966).
7. L. H. Back, P. F. Massier, and R. F. Cuffel, "Measurements of heat exchange in a supersonic nozzle in the zone of separation flow due to a compression shock," Raket. Tekh. Kosmon., No. 5 (1968).
8. V. M. Kudryavtsev, V. A. Burkal'tsev, and M. D. Tumanov, "Heat exchange in overexpanded conical nozzles," Tr. Mosk. Vyssh. Tekh. Uchil., No. 290 (1979).
9. D. R. Bartz, "A simple equation for rapid estimation of rocket nozzle convective heat-transfer coefficients," Jet Propul., 27, 49 (1957).